N91-10488

EXTENDED TIME OBSERVATIONS OF CALIFORNIA MARINE STRATOCUMULUS CLOUDS FROM GOES FOR JULY 1983-1987

Patrick Minnis and Edwin F. Harrison
Atmospheric Sciences Division, NASA Langley Research Center
Hampton, Virginia 23665-5225
and
David F. Young
Aerospace Technologies Division, Planning Research Corporation
Hampton, Virginia 23666

1. Introduction

One of the goals of the First ISCCP Regional Experiment (FIRE) is to relate the relatively small scale (spatial and temporal) Intensive Field Observations (IFO) to larger time and space domains embodied in the Extended Time Observations (ETO) phase of the experiment. The data analyzed here as part of the ETO are to be used to determine some climatological features of the limited area which encompasses the Marine Stratocumulus IFO which took place between 29 June and 19 July 1987 off the coast of southern California (Kloessel et al., 1988).

2. Data and methodology

The primary data for this study are 3-hourly, 8-km visible (0.65 μm) and infrared (10.5 μm) radiances taken by the series of Geostationary Operational Environmental Satellites (GOES) which operated at various longitudinal positions between 1983 and 1987. Analysis of the data was confined to the month of July during each year. Table I lists the satellite, subsatellite longitude, dates of analysis, and satellite viewing zenith angle, VZ, relative to the center of the stratocumulus limited area. The latter is defined by 140°W and 115°W longitudes and 40°N and 25°N latitudes. These bounds were selected to ensure that IFO flight tracks would fall in the domain and that areas with stratocumulus presumably free from continental influences would be included.

The data were analyzed on a 2.5° grid with the hybrid bispectral threshold method described by Minnis et al. (1987). Resulting parameters include cloud amount, cloud-top temperature, cloud albedo, and clear-sky temperature and albedo for each region. All of the cloud parameters were derived for total, low (< 2 km), middle (2-6 km), and high (> 6 km) clouds. Because of the extremely high values (up to 79°) of VZ, the 1987 cloud amounts were adjusted to the viewing angles found for the 1985 data using the technique outlined by Minnis (1988). This correction lowered the cloud amounts by 2-4% absolute cloud amount.

Albedo here refers to the mean top-of-the-atmosphere broadband shortwave (0.2 - 5.0 μm) albedo over clear or cloudy areas. The narrowband visible radiances are converted to broadband radiances using the same conversion formula and coefficients as Minnis et al. (1987) for 1983, 1985, and 1986. That calibration produced good estimates of clear-sky reflectance and consistent mean cloud albedos for all 3 years. The offset voltage remained the same throughout the period.

A different approach was applied for the 1987 GOES-East data since its instruments were different from the previous years (see Table I) and the offset voltage was much lower. The clear-sky visible count (proportional to the square root of radiance) was estimated using the ocean bidirectional model of Minnis and Harrison (1984) calibrated with the same formula used for the previous years. Clear-sky counts over the limited area were also derived from the 1987 GOES-East data. These data were plotted against the calibrated model results and used to fit the GOES-East radiances by forcing the line through the pair of known offset counts. This "calibration" is very uncertain for high radiances but it provides a reasonable estimate of clear-sky reflectance essential for derivation of the cloud parameters. The approach to the calibrations taken here is necessitated by the lack of a consistent calibration source at the present time.

3. Results

All of the results presented here exclude the results for 1984 and 1987 GOES-West since they were unavailable at the time of printing. Figure 1 shows the mean total and layer cloud amounts for the entire period. Mean total cloudiness is less than 70% within 5° of the California coast with the minimum occurring north of 35°N. Cloud cover increases to a maximum between 125°W and 130°W south of 30°N before decreasing to the southwest. Most of the clouds are found in the lowest layer (Fig. 1b), especially in the southern half of the domain. Midlevel and high clouds constitute less than 10% of the total over all marine areas except in the northwest corner (Figs. 1c and 1d). Total cloudiness over the adjacent land areas is less than 30%. The interannual standard deviations of the monthly mean total cloudiness for the period range from 3% in the southwest to nearly 12% over the areas of maximum cloudiness.

The clear-sky temperatures (Fig. 2) over the ocean range from 285K in the north to 290K in the southeast corner of the region. The interannual standard deviations of these temperatures are less than 1K over most of the ocean areas. Values greater than 1K are found over some of the western regions of the grid. Mean equivalent blackbody cloud-top temperatures in Fig. 3 also show a general north-south decrease. The cloud-top isotherms, however, are skewed to the north ridging near the coast while the clear isotherms are more parallel with latitude troughing near the coast. This results in a 1K to 2K east-west gradient in the difference between the two quantities. This difference is about 6K on average indicating that the clouds are confined to the boundary layer as expected. Interannual standard deviations of mean cloud-top temperature range from 0.5K to 1.5K over areas with less than 5% midlevel cloud cover.

Mean clear ocean albedos (Fig. 4) range between 0.10 and 0.12 with standard deviations generally < 0.01. Cloud albedos (Fig. 5) over the ocean regions are typically around 0.35. Maximum marine cloud albedos occur near the coast and along a line southwestward from 35°N, 122°W. Minimum cloud albedo (0.32) is found over the southeastern corner of the region. Interannual standard deviations of cloud albedo vary from less than 0.01 over the northwest corner to 0.06 over the southeastern regions.

Cloud cover over both the marine and land areas undergoes distinct diurnal variations. Over all of the ocean regions, cloud amount peaks between 0300 LST and 0900 LST with a minimum during the afternoon. Two special regions have been defined to determine if any significant differences exist between the diurnal variations of the stratocumulus clouds near the coast and far from the coast. The pacific (PAC) region is a 7.5° box between 32.5°N and 25°N and 140°W and 132.5°W; the IFO region is bordered by 35°N and 30°N and 125°W and 120°W, with an additional 2.5° region to the east centered at 31.3°N and 118.8°W. Figure 6 compares the 3-hourly means for the IFO and PAC. The diurnal range over the PAC is 25%

greater than that near the shore. Minimum cloudiness appears to occur earlier over the PAC and remain longer than it does over the IFO region.

4. Discussion

Cloud amount patterns are similar to those compiled by Sadler et al. (1976). The slightly higher values here may be the result of including night and morning hours in the analysis. Climatological values of sea surface temperatures over the area (Reynolds, 1983) are between 2K and 4K lower than the clear-sky results shown here. The differences which increase from the coast toward the southwest are primarily due to water vapor attenuation and some cloud contamination. Atmospheric moisture variations are probably responsible for the difference gradient. The differences between clear-sky and cloud-top temperatures may be related to the strength of the inversion over the marine boundary layer. Except for the area of maximum albedo extending from the coast, cloud albedos are within 1 - 2% of those found in previous studies (e.g., Minnis et al., 1987) over areas of stratocumulus over the open ocean. The cloud albedo maximum could result from an infusion of continental aerosols near the coast. Diurnal variations of cloudiness are also similar to those found over other parts of the Pacific (e.g., Minnis et al., 1987). Coastal-open ocean differences in the diurnal range may be tied to variations in the strength of the inversion and liquid water content.

5. Concluding remarks

The preliminary results described in this paper provide a long-term perspective of the large-scale cloudiness over the stratocumulus IFO region. Inclusion of data from GOES-West taken during 1984 and 1987 will complete this 5-year climatology of July marine stratocumulus over the IFO limited area. Measurements taken during the IFO will improve our understanding of the behavior of the various parameters observed in this study and over larger time and space scales. This analysis and similar ETO results will provide the link between the IFO and stratocumulus over the rest of the globe and other seasons.

6. References

Kloessel, K. A., B. A. Albrecht, and D. P. Wylie, 1988: FIRE Marine Stratocumulus Observations -- Summary of Operations and Synoptic Conditions. FIRE TR No. 1, 171 pp.

Minnis, P., 1988: Viewing Zenith Angle Dependence of Cloudiness Determined from Coincident GOES-East and GOES-West Data. Submitted to J. Geophys. Res.

Minnis, P. and E. F. Harrison, 1984: Diurnal Variability of Regional Cloud and Clear-Sky Radiative Parameters Derived from GOES Data. Part III: November 1978 Radiative Parameters. J. Clim. Appl. Met., 23, 1033-1051.

Minnis, P., E. F. Harrison, and G. G. Gibson, 1987: Cloud Cover Over the Equatorial Eastern Pacific Derived from July 1983 ISCCP Data Using a Hybrid Bispectral Threshold Method. J. Geophys. Res., 92, 4051-4073.

Reynolds, R. W., 1983: A Comparison of Sea Surface Climatologies. J. Appl. Met., 22, 447-459.

Sadler, J. D., L. Oda, and B. J. Kilonsky, 1976: Pacific Ocean Cloudiness from Satellite Observations. UHMET 76-01, Univ. of Hawaii, Honolulu, 137 pp.

Satellite	Longitude (deg W)	Dates	VZ (deg)
GOES-6	135.0	July 17-31, 1983	39
GOES-6	135.0	July 1-31, 1984	39
GOES-6	108.7	July 1-31, 1985	48
GOES-6	108.7	July 1-31, 1986	48
GOES-7	75.0	July 2-31, 1987	67
GOES-6	135.0	July 1-31, 1987	39

Table 1. Satellite data characteristics. (Note that GOES-6 and GOES-7 are also referred to as GOES-West and GOES-East.)

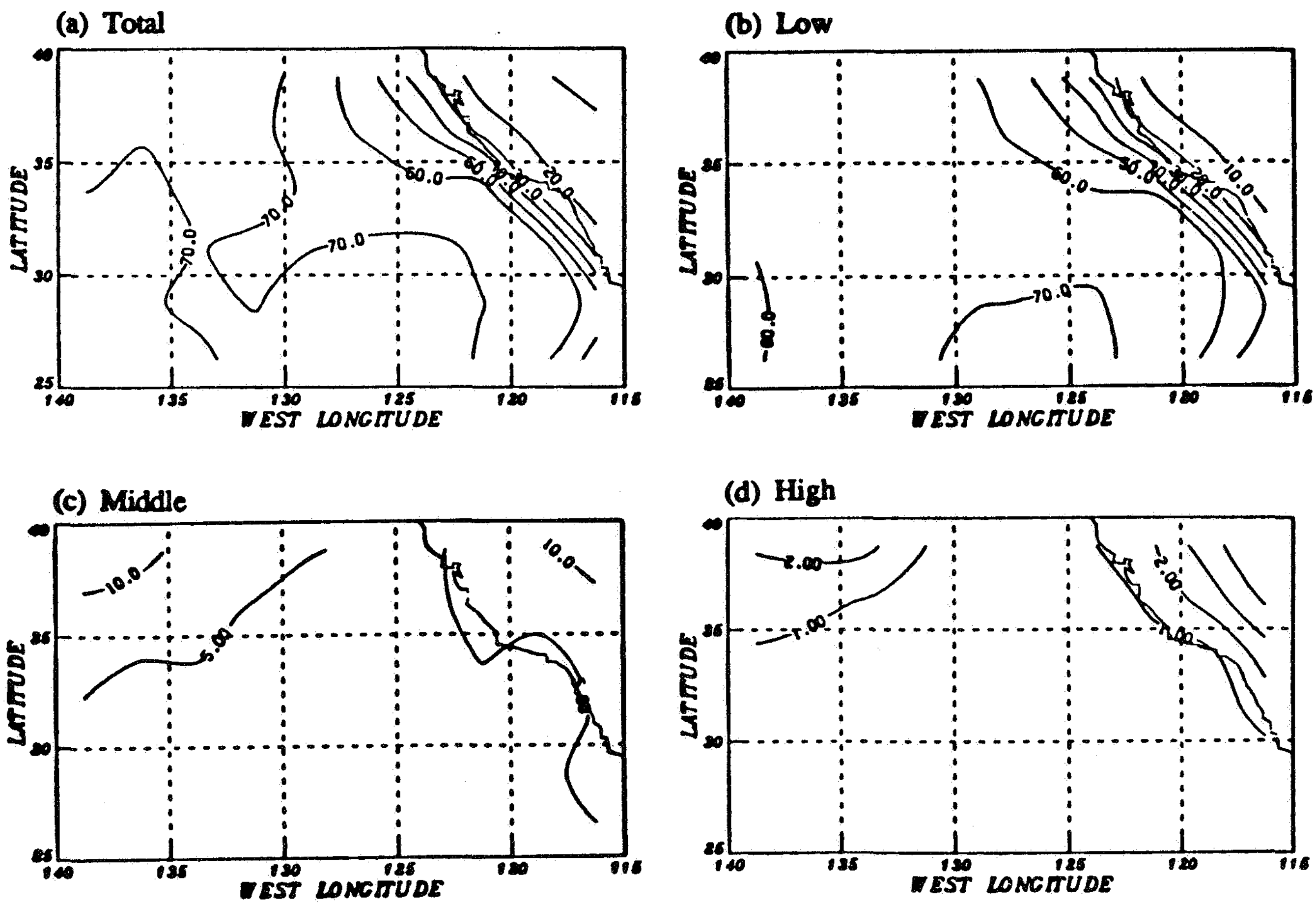

Figure 1. Mean cloud amounts for July (1983 - 1987).

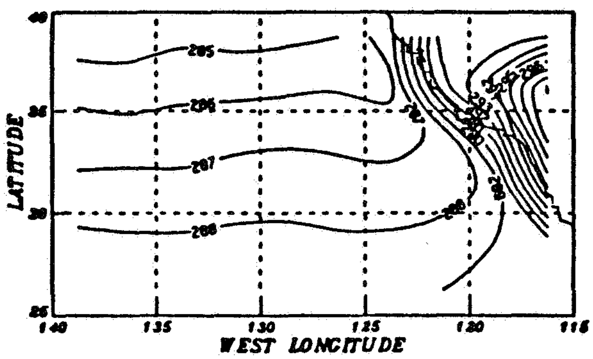

Figure 2. Mean clear-sky temperatures for July (1983 - 1987).

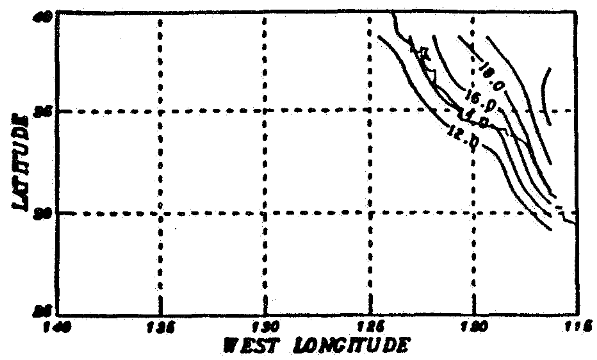

Figure 4. Mean clear-sky albedos for July (1983 - 1987).

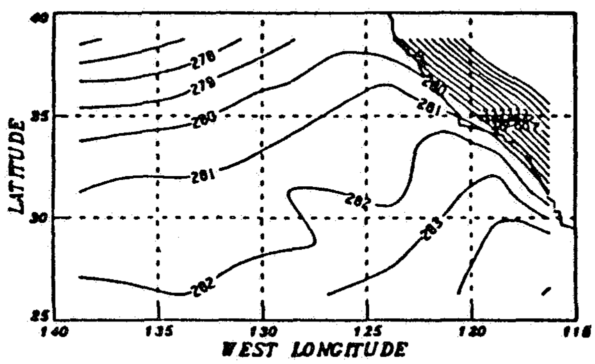

Figure 3. Mean cloud-top temperatures for July (1983 - 1987).

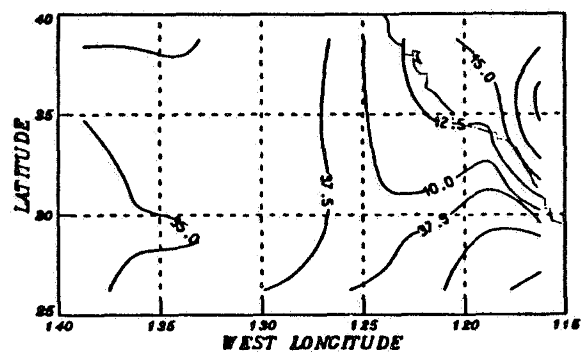

Figure 5. Mean cloud albedos for July (1983 - 1987).

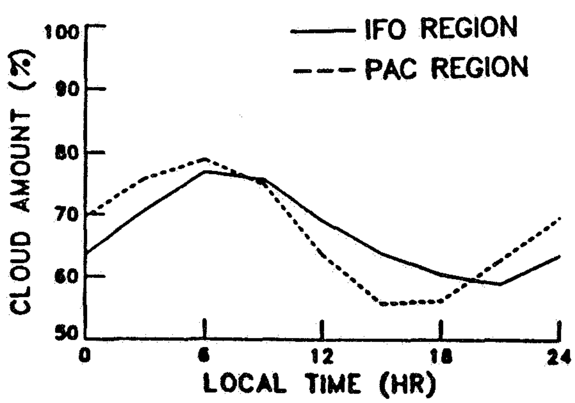

Figure 6. Diurnal variation of cloud cover for July (1983 - 1987).